Metal Induced Specific and Non-specific Oligonucleotide Folding Studied by FRET and Related Biophysical and Bioanalytical Implications

Mehmet Murat Kiy, Zachary E. Jacobi and Juewen Liu[a]*

[a] M.M. Kiy, Z.E. Jacobi, Prof. Dr. J. Liu

Department of Chemistry

Waterloo Institute for Nanotechnology

University of Waterloo, 200 University Avenue West

Waterloo, Ontario, N2L 3G1 (Canada)

Fax: (+1) 519-746-0435

Email: liujw@uwaterloo.ca

Abstract.

Metal induced nucleic acid folding has been extensively studied with ribozymes, DNAzymes, tRNA and riboswitches. These RNA/DNA molecules usually have a high content of double-stranded regions to support a rigid scaffold. On the other hand, such rigid structural features are not available for many *in vitro* selected or rationally designed DNA aptamers; they adopt flexible random coil structures in the absence of target molecules. Upon target binding, these aptamers adaptively fold into a compact structure with a reduced end-to-end distance, making fluorescence resonance energy transfer (FRET) a popular signaling mechanism. However, non-specific folding induced by mono- or divalent metal ions can also reduce the end-to-end distance and thus lead to false positive results. In this study we used a FRET pair labeled Hg^{II} binding DNA and monitored metal induced folding in the presence of various cations. While non-specific electrostatically mediated folding can be very significant, at each tested salt condition, Hg^{II} induced folding was still observed with a similar sensitivity. We also studied the biophysical meaning of the acceptor/donor fluorescence ratio that allowed us to explain the experimental observations. Potential solutions for this ionic strength problem have been discussed. For example, probes designed to signaling the formation of double-stranded DNA showed a lower dependency on ionic strength.

Introduction

In the past several decades, many new functions of nucleic acids have been discovered. Well-known examples include ribozymes and riboswitches, representing the catalytic and molecular recognition functions of RNA, respectively.[1,2] It has been recognized that metal ions often play crucial structural or functional roles in these nucleic acids. Therefore, metal/nucleic acid interaction is one of the frontiers of biophysics and bioinorganic chemistry.[3] Being a polyanion, nucleic acids interact with metal ions through both non-specific electrostatic interactions and site-specific metal coordination; the latter usually has a much higher binding affinity.

Most naturally occurring nucleic acids (e.g. ribozymes, riboswitches, tRNA) possess a rigid structural scaffold with extensive double-stranded regions. In particular, their 3′ and 5′ ends are often base paired even in the absence of ligands. With a protein-like structure, the global folding of these nucleic acids can be probed and non-specific metal-induced condensation often plays a relatively minor role.[4] On the other hand, many *in vitro* selected or rationally designed aptamers are much smaller (e.g. <50 nucleotides) and are present as random coils without a stable secondary structure.[5] Addition of target molecules folds the aptamers into more rigid binding structures (so called adaptive binding), which often accompanies with a reduced end-to-end distance.[5] The adaptive binding property has been used to design fluorescence resonance energy transfer (FRET)-based sensors with end-labeled fluorophores since FRET is known to be sensitive to such distance changes. Many molecules include adenosine/ATP,[6] cocaine,[7] arginiamide,[8] K^{I},[9-12] Mg^{II}/Ca^{II},[13] Ag^{I},[14] Hg^{II},[15,16] thrombin,[17] and (platelet-derived growth factor) PDGF[18,19] have been detected using this method. One particularly interesting example is the Hg^{II} binding DNA shown in Figure 1A. Addition of Hg^{II} folds the DNA into a hairpin.[15,20]

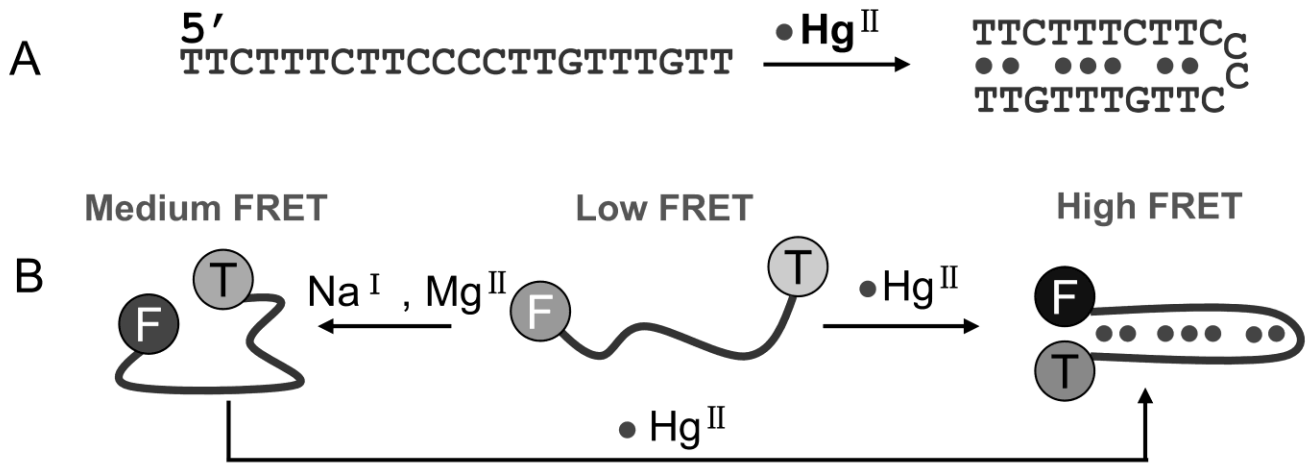

Figure 1. (A) The Hg^{II} binding DNA sequence and its reaction with Hg^{II}. (B) Schematics of DNA conformational change in the presence of Hg^{II} or other metal ions. Without a rigid scaffold, this DNA can fold both through non-specific metal induced condensation and Hg^{II} induced hairpin formation. F and T denote FAM (donor) and TAMRA (acceptor), respectively. Other FRET pairs can also be used.

While effective detection in pure buffers has been achieved, non-specific metal/aptamer interactions may pose significant challenges for practical analytical applications. Without a rigid scaffold, these oligonucleotides can be easily condensed by metal ions such as Na^{I} and Mg^{II},[21-24] which also increases the FRET efficiency and may lead to false positive results (Figure 1B). In other words, the information content from FRET is insufficient to distinguish specific (target induced) and non-specific (metal ion electrostatics related) folding.

In many FRET-related works, the fluorescence intensity ratio of the FRET acceptor over the donor is used for quantification. This ratio is higher for folded DNA as a result of energy transfer. Being convenient for calculation, the biophysical meaning of this ratio related to the DNA end-to-end distance change is often not clear. In this work, we chose to use the Hg^{II} binding DNA as a model to study both non-specific and specific metal-induced folding and to explore its implication in terms of biophysics and analytical chemistry.

Mercury is a highly toxic metal that can cause serious adverse health effects.[25,26] To manage the mercury contamination problem, many sensors have been developed.[27] In particular, a large number of fluorescent,[15,28-30] colorimetric,[31,32] and electrochemical sensors[33,34] have been designed based on the Hg^{II}-thymine binding. In the original paper by Ono *et al*,[15] the DNA shown in Figure 1A was labeled with a 6-carboxyfluorescein (FAM) and a dark quencher (4-(4-dimethylaminophenyl) diazenylbenzoic acid, Dabcyl), respectively on the two ends. Addition of Hg^{II} resulted in DNA hairpin formation and fluorescence quenching. From the analytical chemistry standpoint, this "light-off" sensor has a limited room for signal change and therefore low sensitivity (detection limit = 40 nM Hg^{II}). If the Dabcyl quencher is replaced by another fluorophore such as TAMRA (carboxytetramethylrhodamine) to form a FRET pair with FAM, two important goals can be achieved. First, it is possible to carry out ratiometric detection. Compared to the previous "light-off" design,[15] ratiometric detection allows better reproducibility and higher sensitivity. Second, FRET allows us to quantitatively study DNA folding. In this work, we confirmed that while this DNA probe worked under a wide range of ionic strength conditions, it is difficult to tell whether the signal change was induced by Hg^{II} or other metal ions. Several solutions to this problem have been proposed. This study provides important insights into the folding of such small aptamers and non-structured nucleic acids in general and will aid in the rational design of aptamer-based biosensors.

Results and Discussions

Ratiometric detection. The sequence of the Hg^{II} binding DNA is shown in Figure 1A and each DNA contains seven Hg^{II} binding sites. To achieve ratiometric detection and FRET analysis, its 5′-end was labeled with a FAM and 3′-end with a TAMRA (Figure 1B). In a low salt buffer, the negatively charged DNA was in an extended coil structure with a long FAM-to-TAMRA distance. In the presence of Hg^{II}, the DNA folded into a hairpin and the two fluorophores came close to allow effective energy

transfer. If high concentrations of other metal ions (e.g. Mg^{II} and Na^{I}) were added, the DNA collapsed into a more compact structure due to the screening of the negative charges (but still in random coil), also resulting in a shorter end-to-end distance.[23,35-37] Addition of Hg^{II} to this more compact DNA can still induce the hairpin formation as shown in Figure 1B. However, the amount of distance change might be smaller.

A typical set of fluorescence spectra in the absence and presence of Hg^{II} is shown in Figure 2A. These spectra were collected using 485 nm excitation with 20 nM DNA in buffer (10 mM HEPES, pH 7.6 and 20 mM $NaNO_3$). The 520 nm emission peak results from the direct excitation of FAM, whereas the 580 nm TAMRA peak involved energy transfer. With 80 nM Hg^{II}, the FAM peak decreased while the TAMRA peak increased, indicating increased FRET efficiency. To quantify energy transfer, the fluorescence intensity ratio at 580 over 520 nm (termed FRET ratio in this paper) was often used. A relatively linear increase of this ratio was observed until ~140 nM Hg^{II} (Figure 2B), since each DNA contained seven Hg^{II} binding sites. Although the physical meaning of the FRET ratio is not clear at this moment, it provides a convenient analytical index. Using the 3σ/slope calculation, where σ is the standard deviation for background variation, we achieved a detection limit of 4.0 nM. Therefore, by simply replacing the dark quencher Dabcyl with the FRET acceptor TAMRA, our detection limit improved 10-fold.[15] The main goal of this work is to study the effect of ionic strength on the DNA folding and Hg^{II} detection. To test this, Hg^{II} was titrated from 0 to 80 nM (within the linear range) in different buffers.

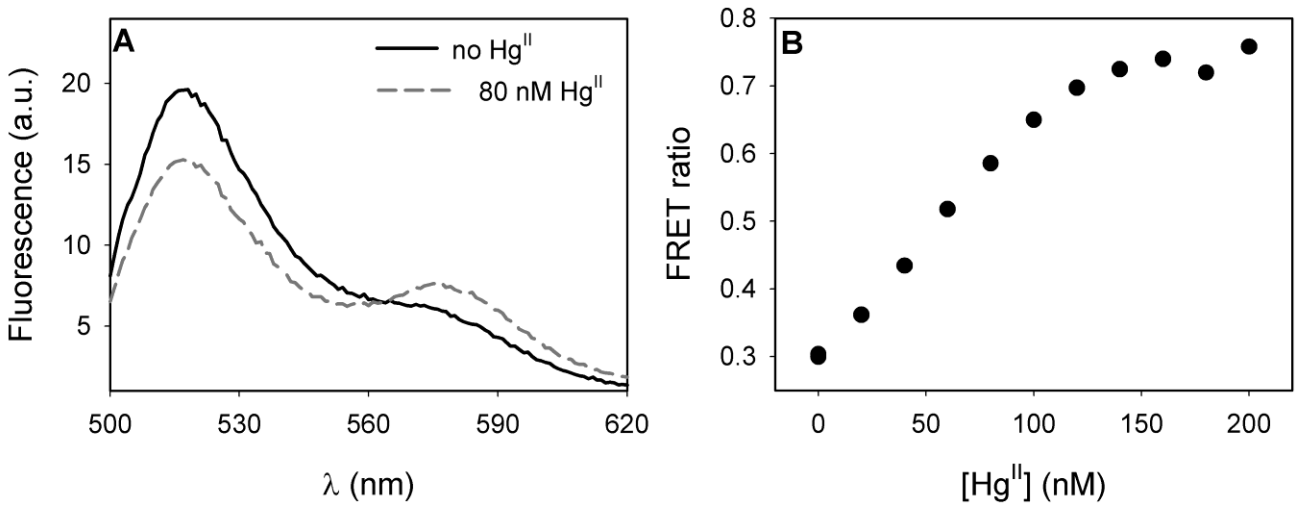

Figure 2. (A). Fluorescence spectra of the Hg^{II} sensor in the presence of 0 and 80 nM Hg^{II} (excitation at 485 nm). (B) FRET ratio (intensity at 580 nm over 520 nm) as a function of Hg^{II} concentration.

Effect of Na^{I}. Since Na^{I} is one of the most commonly encountered metal ions, we first tested its effect. Hg^{II} was titrated to the DNA in the presence of varying concentrations of $NaNO_3$. As can be observed from Figure 3A, the sensor showed a linear response and a similar slope under all tested conditions. The slope of such calibration curves represents sensor sensitivity, which appeared to be independent of Na^{I} up to 500 mM (Figure 3B).

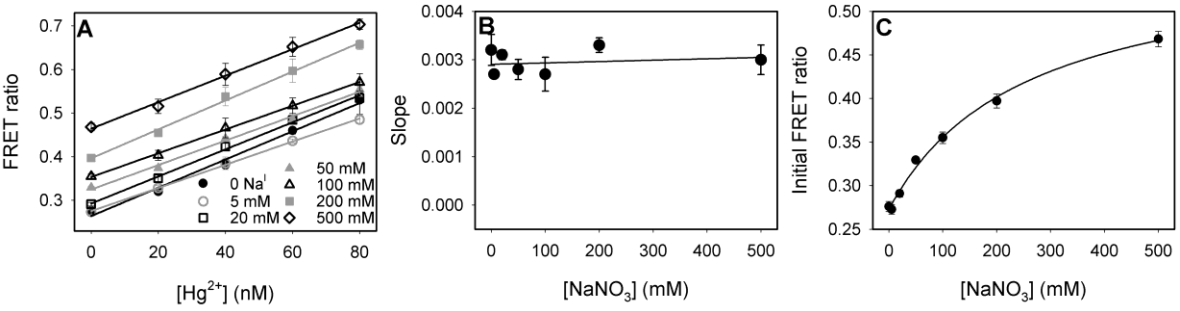

Figure 3. (A) Hg^{II} titration curves in the presence of 0 to 500 mM Na^{I}. (B) The sensitivity (slope) of the titration curves as a function of Na^{I}. (C) The initial FRET ratio of the DNA (in the absence of Hg^{II}) as a function of Na^{I}.

If the initial FRET ratio (no Hg^{II} added) was plotted against $NaNO_3$ concentration in the buffer (Figure 3C), a gradual increase was observed, suggesting that the DNA was folded into a more compact structure in high salt buffers resulting in more energy transfer. Considering that this particular DNA sequence cannot form a stable secondary structure in the absence of Hg^{II}, this Na^{I} induced folding should be due to non-specific electrostatic interactions. An apparent dissociation constant (K_d) of 253 mM Na^{I} was obtained by fitting the data to binding to one Na^{I}, and we consider the physical meaning of this K_d to be the interaction between Na^{I} and the individual phosphates on DNA.

An intriguing observation was that the sensitivity (slope) was independent of Na^{I}, while the initial FRET value was strongly affected. One would predict that with a high value of the initial FRET ratio, the room for its further increase became small and sensitivity should decrease. One explanation is that the Hg^{II}-mediated DNA folding is also stabilized by Na^{I} and there is a synergistic effect between these two metal ions for the hairpin formation. We will also provide a biophysical picture to relate this FRET ratio to the DNA end-to-end distance change, which can also contribute to the observed sensitivity trend (*vide infra*). Analytically, this observation might be useful since the calibration curves have the same slope regardless of the Na^{I} concentration.

Effect of Mg^{II} and Ca^{II}. We next tested divalent ions (Mg^{II} and Ca^{II}) that are commonly used to induce DNA folding. They can either specifically coordinate with nucleic acids or through diffuse binding.[38] Overall a similar pattern was observed as shown in Figure 4A, D; Hg^{II} can still be detected under all of the tested conditions. As shown in Figure 4B, E, the sensitivity became higher with an increasing concentration of these metal ions. The sensitivity improvement reached ~100% in the presence of > 5 mM Ca^{II} (Figure 4B) and was ~50% for Mg^{II} (Figure 4E). Therefore, the overall change in sensitivity was still quite small. Folding induced by Mg^{II} and Ca^{II} occurred with a K_d of ~ 0.6-0.8 mM (black dots, Figure 4C, F), which was over 300-fold tighter than that for Na^{I}. The measurement of the initial FRET ratio showed very good reproducibility and the coefficient of variation was typically smaller than 3%. The slope or sensitivity measurement showed more variability (e.g. close to 20%). Our observation is consistent with the fact that divalent metal ions are much more effective at binding to the phosphate backbone and screen its negative charge. Several transition metal ions were also titrated into the DNA and DNA folding was observed at low μM metal concentrations (see Supporting Information). Therefore, non-specific metal-induced folding of this DNA is a general observation.

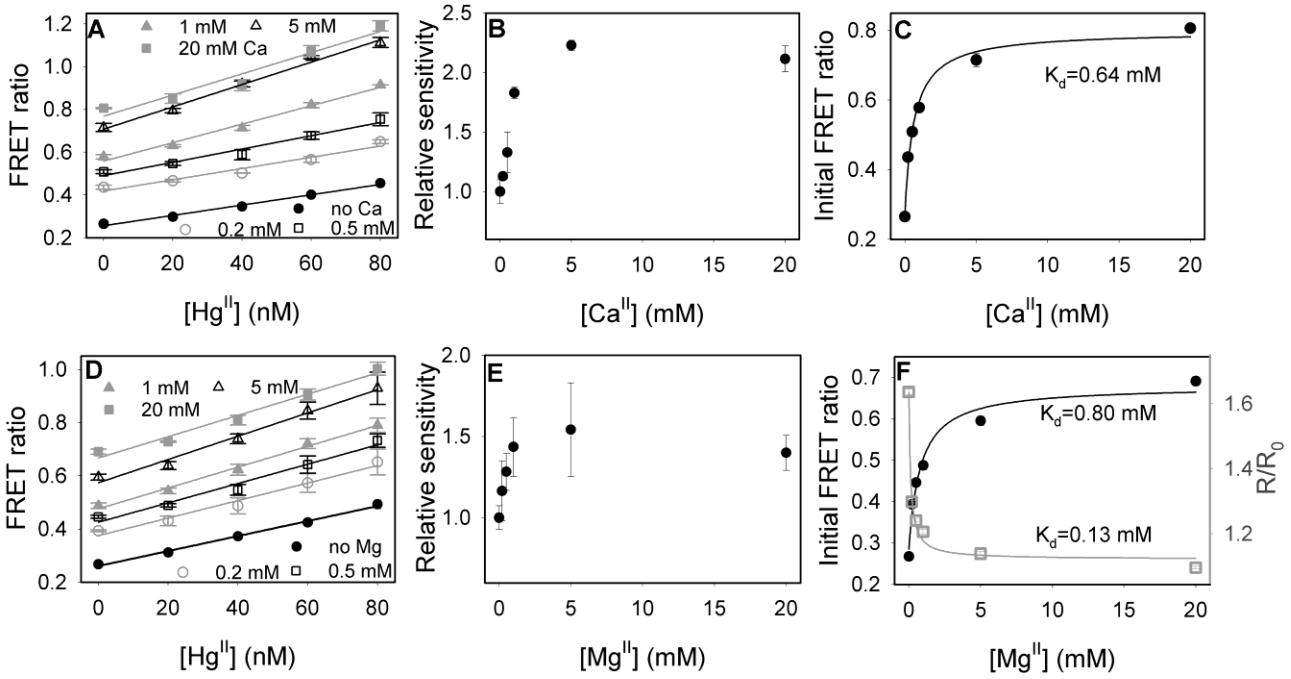

Figure 4. Hg^{II} titration curves in the presence of varying concentrations of Ca^{II} (A) and Mg^{II} (D). The relative sensitivity (slope) of the titration curves as a function of Ca^{II} (B) and Mg^{II} (E). The initial FRET efficiency (black dots) of the DNA (in the absence of Hg^{II}) as a function of Ca^{II} (C) or Mg^{II} (F). The squares in (F) are the change of the end-to-end distance as a function of Mg^{II} concentration. Its *y*-axis is on the right side.

Biophysical meaning of the FRET ratio. From the above experiments, we learned that cations can interfere with Hg^{II} detection by condensing DNA to increase its initial FRET efficiency. At the same time, cations can also facilitate Hg^{II} mediated DNA folding. Using the FRET ratio as the analytical index, the sensor sensitivity either maintained the same value (with Na^{I}) or even improved (with Mg^{II} and Ca^{II}). While using FRET ratio is convenient, its physical meaning is not obvious. To gain a better understanding of DNA folding, we correlated this ratio to the distance change in the Hg^{II} sensor system.

With the 485 nm excitation, the FAM emission at 520 nm in the FRET system was lower compared to that of free FAM because of the presence of the energy acceptor TAMRA; the effect of TAMRA was a quencher for FAM. Therefore, the FAM intensity was proportional to $\varepsilon_{485}^{F}\Phi_{520}^{F}(1-E_T)$, where ε_{485}^{F} and Φ_{520}^{F} were the FAM extinction coefficient at 485 nm and its quantum yield at 520 nm (in the absence of TAMRA), respectively. E_T was the FRET efficiency.[39]

The 580 nm emission peak contained three components. The first was the "red tail" of FAM $\varepsilon_{485}^{F}\Phi_{580}^{F}(1-E_T)$, since the FAM quantum yield at 580 nm (Φ_{580}^{F}) was not zero. The second component was the directly excited TAMRA $\varepsilon_{485}^{T}\Phi_{580}^{T}$, and the final one was the TAMRA emission from energy transfer $\varepsilon_{485}^{F}\Phi_{580}^{T}E_T$. Based on this understanding, we can write the FRET ratio *I* to be:

$$I=\frac{F_{580}}{F_{520}}=\frac{\varepsilon_{485}^{F}\Phi_{580}^{F}(1-E_T)+\varepsilon_{485}^{T}\Phi_{580}^{T}+\varepsilon_{485}^{F}\Phi_{580}^{T}E_T}{\varepsilon_{485}^{F}\Phi_{520}^{F}(1-E_T)}=\frac{\Phi_{580}^{F}}{\Phi_{520}^{F}}+\frac{\Phi_{580}^{T}}{\Phi_{520}^{F}}[\frac{\varepsilon_{485}^{T}}{\varepsilon_{485}^{F}}\frac{1}{(1-E_T)}+\frac{E_T}{(1-E_T)}] \qquad (1)$$

The first term of (1) $\Phi_{580}^{F}/\Phi_{520}^{F}$ =0.14 can be obtained using a FAM-singly labelled sample.

The extinction coefficient ratios of these two fluorophores can be experimentally determined to be $\varepsilon^{T}_{485} / \varepsilon^{F}_{485}$=0.117.[40]

The only unknown was the quantum yield ratio of these two fluorophores $\Phi^{T}_{580} / \Phi^{F}_{520}$. This can be solved by hybridizing the complementary DNA of the Hg^{II} FRET probe to form a 22-mer duplex with a FAM-to-TAMRA distance *R* of ~7.48 ± 0.5 nm. This uncertainty was due to the flexible carbon linker between the fluorophores and the DNA.[41] The Förster distance R_0 of this pair is known to be 5.0 nm,[42] giving an E_T of 0.082 ± 0.031 according to $E_T = R_0^6 /(R_0^6 + R^6)$. The FRET ratio was measured to be 0.297 for this duplex. Bringing the FRET efficiency and FRET ratio of the duplex DNA to (1), we can solve $\Phi^{T}_{580} / \Phi^{F}_{520}$=0.723. Therefore, the FRET ratio can be expressed as

$$I = \frac{F_{580}}{F_{520}} = 0.14 + \frac{0.085}{(1 - E_T)} + \frac{0.723 E_T}{(1 - E_T)} \qquad (2)$$

From (2) we can obtain $E_T = \frac{I - 0.225}{I + 0.583} = \frac{R_0^6}{R_0^6 + R^6}$ and therefore $I = \frac{0.808}{\left(\frac{R}{R_0}\right)^6} + 0.225$ (3)

In Figure 5, the FRET ratio as a function of relative distance change (R/R_0) is plotted. It needs to be noted that the distance *R* here is only an average distance. It is likely that the DNA has a distribution of end-to-end distance due to its non-rigid structure.[43]

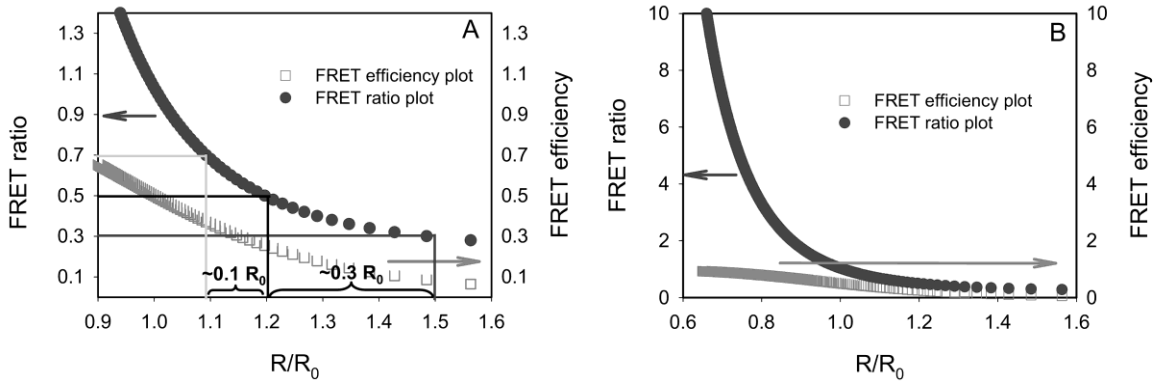

Figure 5. The calculated FRET ratio (left axis) and FRET efficiency (right axis) as a function of end-to-end distance change for the Hg^{II} FRET probe. The distance change was normalized to the Förster distance R_0 of the FAM-TAMRA pair. The FRET ratio change becomes larger at shorter distance. The plots in (A) and (B) were identical except that (B) has a wider distance range than (A). FRET ratio can change from close to 0 to more than 10, but FRET efficiency cannot exceed 1.

The plot in Figure 5A correlates FRET ratio to distance *R*. We can see that when *R* is long (e.g. R = ~1.5R_0 and FRET ratio = ~0.3), a change of 0.2 unit in the FRET ratio corresponds to a large distance change of ~0.3R_0. If *R* was short (e.g. in the presence of Mg^{II} with an initial FRET ratio of 0.5), a 0.2 unit change in the ratio corresponds to a smaller distance change of ~0.1R_0. Therefore, the salt-independent sensitivity can be explained by that although Hg^{II}-induced distance change was smaller in high salt buffers, the FRET ratio change was still large because the ratio was more sensitive to distance change at a shorter distance. It needs to be emphasized that FRET ratio and FRET efficiency are different concepts in this paper. For comparison, we also plotted the FRET efficiency corresponding to the axis on the right in Figure 5. Since FRET efficiency cannot exceed one, it has a smaller room of change; while the FRET ratio can go up quite high at short FAM-to-TAMRA distance (Figure 5B).

After understanding the biophysical meaning of the FRET ratio, we plotted the distance change as a function of Mg^{II} concentration in Figure 4F (squares). We noticed that the distance changed much more sharply than the FRET ratio change. For example, the apparent K_d by fitting the distance change was about 5-fold tighter. This is related to the R^6 relationship between distance and the FRET efficiency. This R^6 relationship also made the standard deviation for distance calculation even smaller (e.g. < 1% in Figure 4F).

Calibrating the ionic strength. From the above examples we can see that the main consequence of ionic strength was the initial FRET ratio, which can easily change several folds. Although the slope of the calibration curves was also influenced by ionic strength, this effect was quite small. Therefore, a

potential solution for this ionic strength problem is to employ a calibration DNA that is insensitive to Hg^{II}. To test this, we designed a DNA sequence that should not bind Hg^{II}, and a scheme of its metal induced folding is presented in Figure 6A. As shown in Figure 6B, indeed, all of the calibration curves in the presence of varying Mg^{II} concentrations were flat (slopes close to zero), but the initial FRET ratio varied significantly (Figure 6C). Within the range of 0 to 5 mM Mg^{II}, the probe was useful for measuring the ionic strength. Practically, however, sensors without calibration are preferred, which require the probing of more specific events beyond the end-to-end distance change.

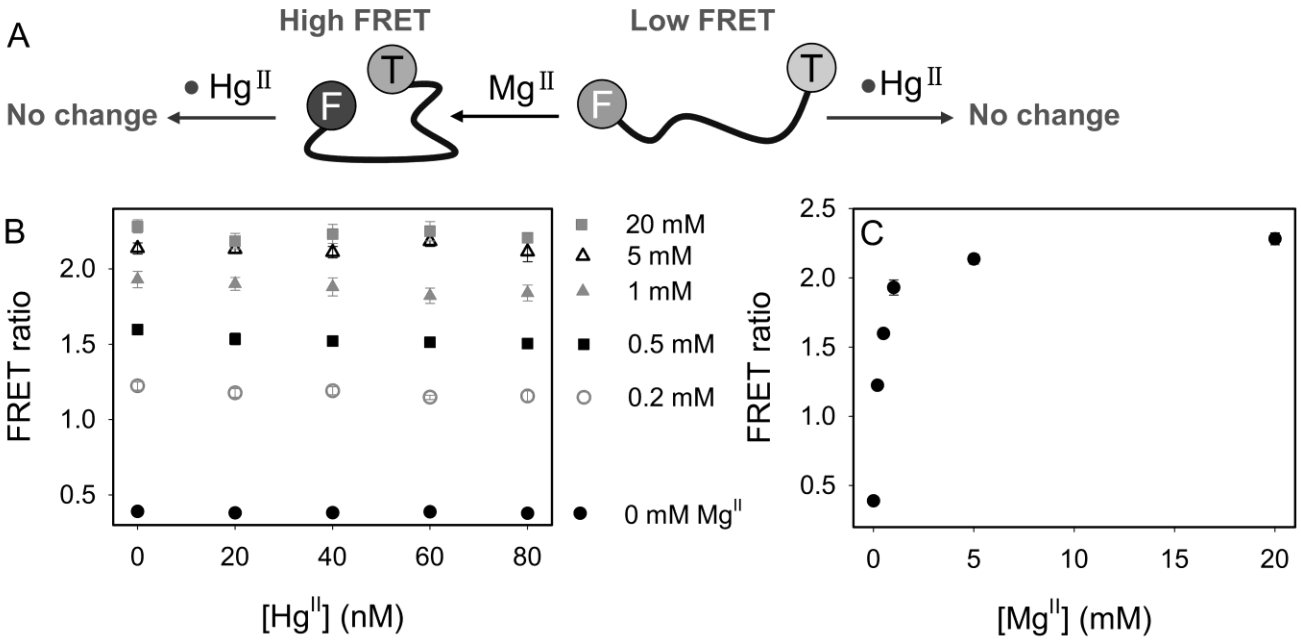

Figure 6. (A) Schematic showing the folding of a random DNA sequence that has no binding affinity for Hg^{II} (only electrostatically mediated folding can occur). F and T denote FAM and TAMRA, respectively. (B) Titration of Hg^{II} to this DNA in the presence of varying concentrations of Mg^{II}. (C) The initial FRET ratio of this DNA as a function of Mg^{II}.

Probing more specific events. The FRET-based sensor measures only the end-to-end distance, whose change can be attributed to both specific and non-specific metal binding. Hg^{II} mediated DNA folding is accompanied by the formation of DNA base pairs, which is not likely to be the case for non-specific

metal-induced DNA condensation. This difference might be harnessed to reduce the effect of solution ionic strength. For example, DNA binding dyes such as SYBR Green I (SG) have also been used to design Hg^{II} sensors.[28,30,44,45] Hg^{II} induced DNA hairpin formation, upon which SG can bind to increase its fluorescence (Figure 7A). Fluorescence spectra of the sensor in the absence and presence of Hg^{II} are shown in Figure 7B and the increase of the fluorescence intensity can be observed. The Hg^{II} titration experiment was carried out in buffers containing varying concentrations of Mg^{II}. As shown in Figure 7C, the calibration curves overlapped in the range of 0 to 1 mM Mg^{II}, confirming that by probing the formation of DNA duplex, salt related artifacts can be minimized. At even higher Mg^{II} concentrations, the overall fluorescence dropped due to quenching of SG fluorescence by Mg^{II}.[46]

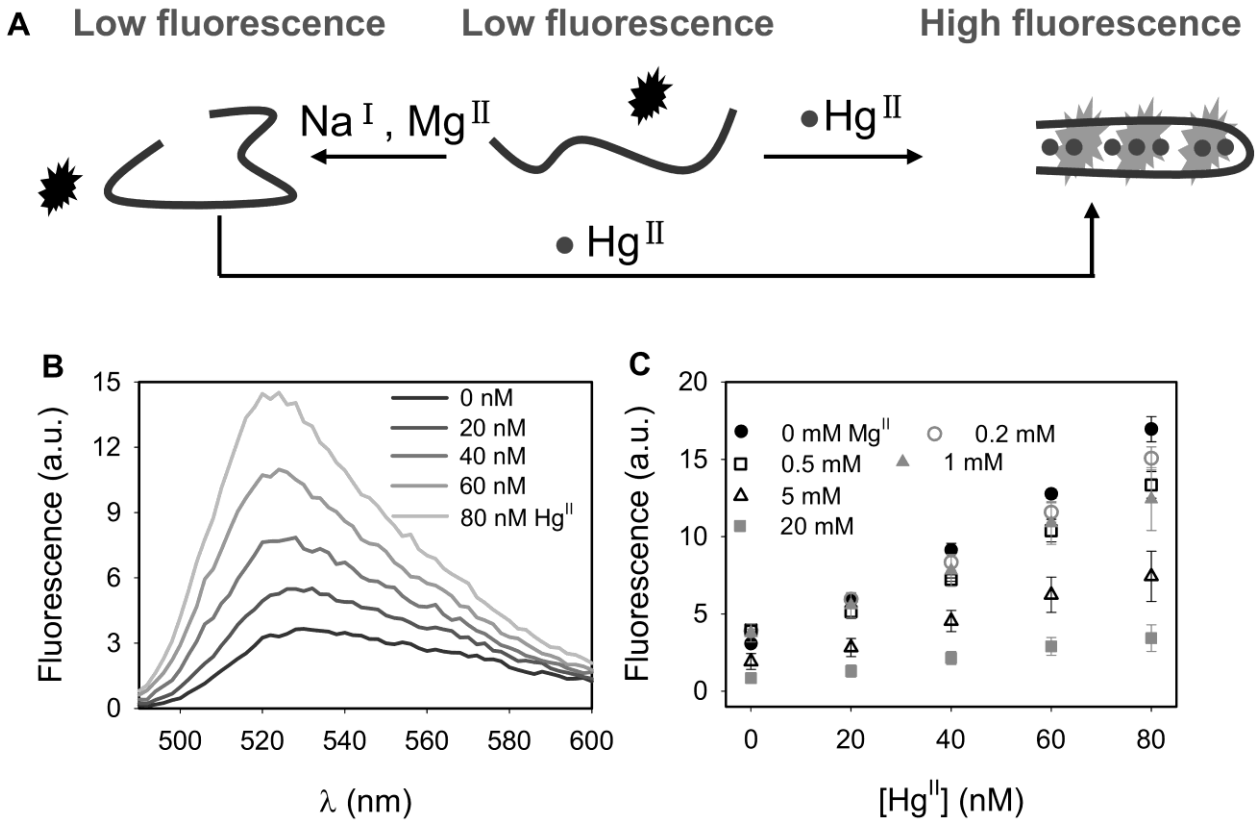

Figure 7. (A) Schematic showing SG-based Hg^{II} detection. Non-specific DNA folding does not result in DNA base pair formation and thus no signal was generated in the presence of SG. (B) Fluorescence spectra of the sensor (in 10 mM HEPES, pH 7.6, no additional salt) in the presence of varying

concentrations of Hg^{II}. (C) Fluorescence measured upon adding Hg^{II} to the DNA sensor in the presence of varying concentrations of Mg^{II}.

The ionic strength problem stems from the lack of a rigid structural scaffold in this probe. As mentioned previously, this is less of a problem for naturally occurring functional nucleic acids. For example, large ribozymes,[47-49] riboswitches,[50] as well as small functional nucleic acids including transfer RNA,[51] small ribozymes,[52,53] and DNAzymes[54,55] contained a relatively rigid structure with extensive double-stranded regions. Analytical chemists have also designed similar sensors. For example, short antisense DNAs were employed to rigidify aptamer backbones and a DNAzyme scaffold was also used. In these so-called structure switching aptamers[29,56,57] or allosteric DNAzymes,[58] although the effect of non-specific DNA folding was reduced, other effects related to the ionic strength, such as the stability of the DNA duplex may still have to be considered.

Fortunately, for a given sample type, the ionic strength is relatively well-defined. For example, the calcium concentration in Lake Ontario changed only less than 20% in the past 40 years.[59] Therefore, sensor design can be optimized for these specific applications. The standard addition method can also be used to further minimize such sample matrix effect. For an unknown sample, however, the possibility of false signals resulting from non-specific DNA folding needs to be taken into consideration.

Conclusions.

In summary, we studied an important but often underexplored area of metal/DNA interaction. Using an oligonucleotide that can fold into a specific structure by Hg^{II}, we demonstrated the effect of ionic strength on its folding. Many aptamers obtained from *in vitro* selection have a similar random coil structure in solution. Therefore, non-specific metal-induced DNA folding or condensation can readily occur, leading to false positive signals for sensors designed to monitor the end-to-end distance change.

We discussed solutions to this problem either using a calibration DNA for ionic strength, probing more specific events, or introducing a more rigid structural scaffold. We also elucidated the biophysical meaning of the FRET ratio that is often used for quantification in FRET-based sensors. Important biophysical insights in terms of metal-induced end-to-end distance change were obtained based on these understandings. In this work, we considered only the effect of several metal ions. Other cationic species such as polyamines, cationic peptides and proteins may also present in various samples. Such polycations are known to strongly bind and condense even double-stranded nucleic acids and are likely to also interfere with the performance of aptamer sensors. Their effect will be a topic of future studies.

Experimental Section

Chemicals. The FAM and TAMRA dual labeled DNAs were purchased from GeneLink (Hawthorne, NY) and were gel purified by the vendor. The random DNA sequence for calibrating the ionic strength is 5′-FAM–ACGCATCTGTGAAGAGAACCTGGA–TAMRA. The sequence for the Hg^{II} probe is 5′-FAM–TTCTTTCTTCCCCTTGTTTGTT–TAMRA. The unmodified Hg^{II} binding DNA and its complementary DNA were purchased from Integrated DNA Technologies (Coralville, IA). Sodium nitrate and 4-(2-hydroxyethyl)-1-piperazineethanesulfonic acid (HEPES) were purchased from Mandel Scientific (Guelph, Ontario, Canada). 10,000× SYBR Green I in dimethyl sulfoxide (DMSO) was purchased from Invitrogen. The nitrate salts of Ca^{II} and Mg^{II} were purchased from Fisher; and $Hg(ClO_4)_2$, $CdCl_2$, $CuSO_4$, $ZnCl_2$, and $Pb(OAc)_2$ were purchased from Sigma-Aldrich at the highest available purity.

Metal titration to the FRET-based sensors. The titration experiments were carried out in a quartz cuvette with a sample volume of 500 μL at room temperature using a Varian Eclipse fluorometer. The excitation wavelength was set at 485 nm and emission was scanned from 500 to 620 nm. All of the titrations were run in triplicates. For each sample, the cuvette contained 498 μL of 10 mM HPEPS, pH

7.6 with varying concentrations of salt and 2 μL of 5 μM dual-labeled DNA to achieve a DNA concentration of 20 nM. After this, 10 μM Hg^{II} was titrated in increments of 1 μL to achieve a final Hg^{II} concentration of 20 to 80 nM. Fresh mercury dilutions using 1 mM HNO_3 were made about once every week from a 10 mM stock dissolved in 100 mM HNO_3.

Hg^{II} titration to the SYBR Green I (SG)-based sensor. For this experiment, the cuvette contained 20 nM unmodified DNA and 120 nM SG in 10 mM HEPES, pH 7.6 with different Mg^{II} concentrations. The excitation wavelength was 480 nm and the emission was recorded from 490 to 600 nm at room temperature. The same concentrations of Hg^{II}, as mentioned above, were added.

Acknowledgments. Funding for this work is from the University of Waterloo, the Canadian Foundation for Innovation, Ontario ministry of Research and Innovation, and the Discovery Grant of the Natural Sciences and Engineering Research Council (NSERC) of Canada.

References:

[1] J. A. Doudna, T. R. Cech, *Nature* **2002**, *418*, 222-228.

[2] R. R. Breaker, *Nature* **2004**, *432*, 838.

[3] A. M. Pyle, *J. Biol. Inorg. Chem.* **2002**, *7*, 679-690.

[4] M. Steiner, D. Rueda, R. K. O. Sigel, *Angew. Chem., Int. Ed.* **2009**, *48*, 9739-9742.

[5] T. Hermann, D. J. Patel, *Science* **2000**, *287*, 820-825.

[6] H. Urata, K. Nomura, S.-i. Wada, M. Akagi, *Biochem. Biophys. Res. Comm.* **2007**, *360*, 459-463.

[7] M. N. Stojanovic, P. de Prada, D. W. Landry, *J. Am. Chem. Soc.* **2001**, *123*, 4928-4931.

[8] H. Ozaki, A. Nishihira, M. Wakabayashi, M. Kuwahara, H. Sawai, *Bioorg. Med. Chem. Lett.* **2006**, *16*, 4381.

[9] H. Ueyama, M. Takagi, S. Takenaka, *J. Am. Chem. Soc.* **2002**, *124*, 14286-14287.

[10] S. Nagatoishi, T. Nojima, E. Galezowska, A. Gluszynska, B. Juskowiak, S. Takenaka, *Anal. Chim. Acta* **2007**, *581*, 125-131.

[11] S. Nagatoishi, T. Nojima, E. Galezowska, B. Juskowiak, S. Takenaka, *ChemBioChem* **2006**, *7*, 1730-1737.

[12] S. Nagatoishi, T. Nojima, B. Juskowiak, S. Takenaka, *Angew. Chem., Int. Ed.* **2005**, *44*, 5067.

[13] T. M. Lerga, C. K. O'Sullivan, *Anal. Chim. Acta* **2008**, *610*, 105-111.

[14] A. Ono, S. Cao, H. Togashi, M. Tashiro, T. Fujimoto, T. Machinami, S. Oda, Y. Miyake, I. Okamoto, Y. Tanaka, *Chem. Comm.* **2008**, 4825-4827.

[15] A. Ono, H. Togashi, *Angew. Chem., Int. Ed.* **2004**, *43*, 4300-4302.

[16] L. Guo, N. Yin, G. Chen, *J. Phys. Chem. C* **2011**, *115*, 4837-4842.

[17] J. J. Li, X. Fang, W. Tan, *Biochem. Biophys. Res. Comm.* **2002**, *292*, 31-40.

[18] C. J. Yang, S. Jockusch, M. Vicens, N. J. Turro, W. Tan, *Proc. Natl. Acad. Sci. U.S.A.* **2005**, *102*, 17278-17283.

[19] M. C. Vicens, A. Sen, A. Vanderlaan, T. J. Drake, W. Tan, *ChemBioChem* **2005**, *6*, 900-907.

[20] Y. Miyake, H. Togashi, M. Tashiro, H. Yamaguchi, S. Oda, M. Kudo, Y. Tanaka, Y. Kondo, R. Sawa, T. Fujimoto, T. Machinami, A. Ono, *J. Am. Chem. Soc.* **2006**, *128*, 2172.

[21] R. K. O. Sigel, H. Sigel, *Acc. Chem. Res.* **2010**, *43*, 974-984.

[22] E. Freisinger, R. K. O. Sigel, *Coord. Chem. Rev.* **2007**, *251*, 1834-1851.

[23] K. M. Parkhurst, L. J. Parkhurst, *Biochemistry* **1995**, *34*, 293-300.

[24] B. Juskowiak, *Anal. Chim. Acta* **2006**, *568*, 171-180.

[25] J. G. Dorea, C. M. Donangelo, *Clin. Nutr.* **2006**, *25*, 369-376.

[26] P. B. Tchounwou, W. K. Ayensu, N. Ninashvili, D. Sutton, *Environ. Toxicol.* **2003**, *18*, 149-175.

[27] E. M. Nolan, S. J. Lippard, *Chem. Rev.* **2008**, *108*, 3443-3480.

[28] J. Wang, B. Liu, *Chem. Comm.* **2008**, 4759-4761.

[29] Z. Wang, J. H. Lee, Y. Lu, *Chem. Comm.* **2008**, 6005-6007.

[30] C. K. Chiang, C. C. Huang, C. W. Liu, H. T. Chang, *Anal. Chem.* **2008**, *80*, 3716-3721.

[31] J.-S. Lee, M. S. Han, C. A. Mirkin, *Angew. Chem., Int. Ed.* **2007**, *46*, 4093-4096.

[32] D. Li, A. Wieckowska, I. Willner, *Angew. Chem. Int. Ed.* **2008**, *47*, 3927-3931.

[33] S.-J. Liu, H.-G. Nie, J.-H. Jiang, G.-L. Shen, R.-Q. Yu, *Anal. Chem.* **2009**, *81*, 5724-5730.

[34] R.-M. Kong, X.-B. Zhang, L.-L. Zhang, X.-Y. Jin, S.-Y. Huan, G.-L. Shen, R.-Q. Yu, *Chem. Comm.* **2009**, 5633-5635.

[35] M. J. Stevens, S. J. Plimpton, *Eur. Phys. J. B* **1998**, *2*, 341-345.

[36] C. D. Downey, J. L. Fiore, C. D. Stoddard, J. H. Hodak, D. J. Nesbitt, A. Pardi, *Biochemistry* **2006**, *45*, 3664-3673.

[37] B. I. Kankia, L. A. Marky, *J. Am. Chem. Soc.* **2001**, *123*, 10799-10804.

[38] V. K. Misra, D. E. Draper, *Biopolymers* **1998**, *48*, 113.

[39] R. M. Clegg, *Meth. Enzymol.* **1992**, *211*, 353-388.

[40] J. Liu, Y. Lu, *J. Am. Chem. Soc.* **2002**, *124*, 15208-15216.

[41] T. L. Jennings, M. P. Singh, G. F. Strouse, *J. Am. Chem. Soc.* **2006**, *128*, 5462-5467.

[42] M. Lorenz, A. Hillisch, S. Diekmann, *Rev. Mol. Biotechnol.* **2002**, *82*, 197-209.

[43] T. H. Evers, E. M. W. M. van Dongen, A. C. Faesen, E. W. Meijer, M. Merkx, *Biochemistry* **2006**, *45*, 13183-13192.

[44] N. Dave, P.-J. J. Huang, M. Y. Chan, B. D. Smith, J. Liu, *J. Am. Chem. Soc.* **2010**, *132*, 12668–12673.

[45] K. A. Joseph, N. Dave, J. Liu, *ACS Appl. Mater. Inter.* **2011**, *3*, 733–739.

[46] H. Zipper, H. Brunner, J. Bernhagen, F. Vitzthum, *Nucleic Acids Res.* **2004**, *32*, e103.

[47] R. Hanna, J. A. Doudna, *Curr. Opin. Chem. Biol.* **2000**, *4*, 166-170.

[48] R. K. O. Sigel, *Eur. J. Inorg. Chem.* **2005**, 2281-2292.

[49] R. K. O. Sigel, A. M. Pyle, *Chem. Rev.* **2007**, *107*, 97.

[50] J. F. Lemay, J. C. Penedo, R. Tremblay, D. M. J. Lilley, D. A. Lafontaine, *Chem. Biol.* **2006**, *13*, 857-868.

[51] V. K. Misra, D. E. Draper, *J. Mol. Biol.* **2000**, *299*, 813-825.

[52] V. J. DeRose, *Curr. Opin. Struct. Biol.* **2003**, *13*, 317-324.

[53] C. Hammann, D. M. J. Lilley, *ChemBioChem* **2002**, *3*, 690-700.

[54] H. K. Kim, I. Rasnik, J. W. Liu, T. J. Ha, Y. Lu, *Nat. Chem. Biol.* **2007**, *3*, 762-768.

[55] H.-K. Kim, J. Liu, J. Li, N. Nagraj, M. Li, C. M. B. Pavot, Y. Lu, *J. Am. Chem. Soc.* **2007**, *129*, 6896-6902.

[56] R. Nutiu, Y. Li, *Chem. Eur. J* **2004**, *10*, 1868-1876.

[57] R. Nutiu, Y. Li, *J. Am. Chem. Soc.* **2003**, *125*, 4771-4778.

[58] J. Liu, Y. Lu, *Angew. Chem., Int. Ed.* **2007**, *46*, 7587-7590.

[59] A. Dove, *Aquat. Ecosyst. Health.* **2009**, *12*, 281-295.